Theoretical study of atomic transport via interstitials in dilute Fe-P alloys

E. Meslin,[1] Chu-Chun Fu,[1] A. Barbu,[1] F. Gao,[2] and F. Willaime[1]
[1]*Service de Recherches de Métallurgie Physique, CEA/Saclay, 91191 Gif-sur-Yvette Cedex, France*
[2]*Pacific Northwest National Laboratory, Richland, Washington 99352, USA*
(Received 16 June 2006; revised manuscript received 30 November 2006; published 20 March 2007)

By combining density functional theory, empirical potential, and atomic transport model approaches, we investigate the energetics and the diffusion properties of P interstitials in dilute Fe-P alloys. Although P is a substitutional impurity in α-iron, when a self-interstitial atom (SIA) approaches a substitutional P, the P atom becomes interstitial with an energy gain of up to 1.0 eV. The octahedral and the $\langle 110 \rangle$ mixed dumbbell are the lowest-energy configurations with similar stabilities. The P atoms are highly mobile in both configurations. The transitions between these two configurations also require low activation energies. The most likely mechanisms leading to long-distance diffusion of a P interstitial are proposed by *ab initio* calculations. The resulting effective diffusion energy estimated by the transport model is 0.19 eV, which agrees with the result from resistivity recovery experiments, suggesting that the Fe-P mixed dumbbells are more mobile than the SIAs. The fast-migrating P interstitial can be deeply trapped by a substitutional P atom. The resulting complexes are very stable with a binding energy of around 1.0 eV. Their mobilities are investigated by means of the dimer method using an Fe-P empirical potential. A comparison between the present predictions and existing experimental results is also discussed.

DOI: 10.1103/PhysRevB.75.094303 PACS number(s): 72.25.Ba, 61.72.−y, 71.15.Mb, 61.80.−x

I. INTRODUCTION

The embrittlement of reactor pressure vessel (RPV) steels may be partly due to the intergranular segregation of solute atoms which weakens the grain boundary cohesion. After thermal aging, P segregation is driven by thermodynamical forces. A decrease in free energy associated with phosphorus atoms moving toward grain boundaries has been noted around 450 °C. However, the phosphorus mobility is too low to produce a significant segregation at 300 °C or below. Under irradiation, the ductile-brittle transition temperature has been shown to increase by the Charpy test.[1] Enhancement of phosphorus intergranular segregation in ferritic steels such as E911 has been evidenced by field emission gun scanning transmission electron microscopy.[2] A small increase in phosphorus concentration at grain boundaries in RPV steels has also been observed experimentally.[1] Two mechanisms may explain the segregation of phosphorus under irradiation. Indeed, not only are supersaturation of vacancies and self-interstitial atoms (SIAs) induced, but also fluxes of point defects moving toward grain boundaries and dislocation loops. The former can enhance P segregation driven by the same thermodynamic force as under thermal aging. In addition, point defect flux may also induce segregation due to flux coupling between the point defect and phosphorus;[3,4] the corresponding driving force is purely kinetic.

In order to understand the irradiation effect on the intergranular phosphorus segregation in steels, accurate knowledge of the interaction between P and point defects, P diffusion mechanisms, and the kinetics of P segregation are required.

Atomistic simulations based on empirical interatomic potentials[5–7] were carried out to address these issues. Information has been obtained concerning the mobility of P atoms and their interaction with radiation defects.[8–10] Hurchand *et al.* studied the energetics of P atoms at grain boundaries,[11] and Barashev showed that vacancies can drag P atoms toward sinks of point defects.[12] These studies are much less computationally demanding than *ab initio* calculations, but the predictive power of their results is restricted to the validity of the interatomic potential used.

A recent *ab initio*-based work by Domain and Becquart[13] devoted to the study of the energetics of P atoms in α-iron showed that P atoms interact strongly with both vacancies and SIAs. Phosphorus migration energies associated with diffusion by the vacancy mechanism have also been reported.

Lidiard[14] used an analytic atomic transport model by Barbu and Lidiard[15] to estimate the diffusion coefficients (D) related to the phosphorus diffusion in ferritic steels. The input parameters were derived from data fitted to experimental results by Druce *et al.*[16] The binding energy of the Fe-P mixed dumbbell was found to be 0.17 eV, which is much lower than the value from *ab initio* calculations.[7,13] Furthermore, as pointed out by Lidiard,[14] this approach also failed in predicting the trapping of SIAs proposed by Hardouin-Duparc and Barbu[17] to explain the strong effect of phosphorus on the nucleation of interstitial loops in electron-irradiated steels.

Despite the previous efforts, the detailed behavior of phosphorus in ferritic steels is not yet fully established. In particular, information about the diffusion properties of P atoms via interstitial mechanisms, which may play a central role on the intergranular segregation kinetics under irradiation, is still missing.

Here we investigate, by means of an *ab initio* method, the stability and the migration properties of a phosphorus atom in various interstitial positions. Complementary dimer-method calculations[18] using embedded atom model (EAM) potentials[7] are also performed for a systematic search of possible migration paths. The obtained energetic and migration properties were then introduced as input data into a modified

version of the atomic transport model for dilute bcc alloys. The results are discussed in the light of existing experimental evidence.

II. METHODOLOGY

A. *Ab initio* method

The present *ab initio* calculations have been performed within the density functional theory (DFT) as implemented in the SIESTA code.[19] The calculations are spin polarized and use the generalized gradient approximation (GGA). Core electrons are replaced by nonlocal norm-conserving pseudopotentials while valence electrons are described by linear combinations of numerical pseudoatomic orbitals. The pseudopotential and the basis set for Fe atoms are the same as in Ref. 20. The cutoff radius for the pseudopotential of P is set to 0.99 Å, and its basis set consists in two localized functions for the 3*s* states and six for the 3*p* states. The cutoff radii are 2.67 and 3.34 Å, respectively. Five functions for the 3*d* states are included as polarized orbitals in order to increase angular flexibility. The charge density is represented on a regular real space grid of 0.078 Å. The present approach has been shown to successfully account for the properties of defects in iron:[20–22] the accuracies of the Fe pseudopotential and basis set have been tested on relevant bulk and vacancy properties, and shown to agree satisfactorily with experimental and plane wave DFT GGA values.[20] The validity of the P description is shown in this work through a comparison with plane wave results.

Supercell calculations were performed to study the defect properties. Results have been obtained on 128 and 250 atom cells using $3\times3\times3$ and $2\times2\times2$ shifted *k*-point grids, respectively. The Methfessel-Paxton broadening scheme with a 0.3 eV width was used. Calculated defect energies have been verified to be well converged with respect to these *k*-point grids as shown below. We have performed constant-pressure calculations to estimate P energetics in various configurations, i.e., the structures were optimized by relaxing both the atomic positions and the shape and volume of the supercell. The migration paths have been calculated at constant volume using the drag method in a similar fashion as in Refs. 20–22: for a given reaction coordinate, the atomic positions relative to the center of mass are constrained to relax within the corresponding hyperplane perpendicular to the vector connecting the initial and final positions. Some relevant migration paths have also been checked using the more general nudged elastic band method; the results from both methods are found to be in excellent agreement.[23]

B. Dimer method for systematic finding of saddle points

Possible transitions starting from the most relevant P interstitial positions were systematically searched for using the dimer method. Due to the high computational cost of such calculations at the *ab initio* level, a newly developed Fe-P EAM potential[7] was used. This approach is useful to suggest possible migration paths to be further validated by *ab initio* studies. The dimer method is described in detail elsewhere.[18] It is different from other widely used saddle-point-searching algorithms, e.g., the drag and the nudged elastic band method, in the sense that only knowledge of the initial state is required. The transition states and jump mechanisms of P interstitials were studied using a cubic supercell containing 2000 atoms with periodic boundary conditions. All the atoms in the cell are free to move and relax during the dimer search. The dimer separation was set to 10^{-3} Å, and the values of the finite difference steps for rotation and translation are 10^{-4} and 10^{-3} Å, respectively. The maximum move distance for the dimer has been set to 0.005 Å, which is smaller than the value used in Ref. 24, in order to obtain a higher success rate of 90%. The search was stopped when the maximum force component of the atoms was less than 10^{-4} eV/Å. 100 dimer searches have been carried out starting from each initial state, and the initial dimer vectors were generated randomly to have nonzero components on only 20–50 atoms around the P interstitial atom.

C. Atomic transport model

The atomic transport model used here is derived from the model by Barbu and Lidiard.[15] Modifications have been done according to information provided by the present *ab initio* results on the P migration barriers. This model is based on the Franklin and Lidiard theory of atomic transport.[25] In this study, we have considered only the SIAs and the solute fluxes J_I and J_P. The corresponding equations have the following Fick-like form:

$$\frac{1}{n}J_I = -D_I \nabla c_I' - D_{PI}^I c_P' \nabla c_I' - D_{IP}^I c_I' \nabla c_P', \tag{1}$$

$$\frac{1}{n}J_P = -D_{IP}^P c_I' \nabla c_P' - D_{PI}^P c_P' \nabla c_I', \tag{2}$$

where n is the number of lattice sites per unit volume, c_I' and c_P' are the fractional concentrations of free self-interstitials and phosphorus atoms, respectively, D_I is the diffusion coefficient of SIAs, and D_{IP} and D_{PI} are the kinetic cross coefficients.

III. RESULTS AND DISCUSSION

A. Stability of P interstitial in α-iron

Phosphorus is a substitutional impurity in α-iron. Although it is smaller than the Fe atom, its atomic volume in the bcc iron matrix is very close to that of a Fe atom. Inward relaxation amplitudes of the first neighbors of a substitutional P atom (P_{sub}) are less than 0.3% of the nearest neighbor distance. The interstitial sites are indeed energetically less favorable; their formation energies are at least 2.8 eV higher than that of a substitutional site. However, when a SIA is formed, e.g., under irradiation conditions, and approaches a substitutional P atom, a "kick-out" reaction is expected to occur, which creates a P interstitial (P_{int}), and this $P_{sub}+SIA \rightarrow P_{int}$ reaction induces a large energy gain (binding energy), up to 1.0 eV.

The relative stabilities of the high-symmetry P_{int} configurations are studied by calculating the respective formation

TABLE I. Formation and binding energies (values in parentheses) with respect to dissociation into P_{sub} and $\langle 110\rangle_{Fe\text{-}Fe}$ of P interstitials in iron calculated using three conditions as described in Sec. III B: (i) N_{CV}, (ii) $N+1_{CV}$, and (iii) N_{CP}, where $N=128$ or 250, and CV and CP denote constant-volume and constant-pressure calculations, respectively. The present SIESTA values are compared with the VASP (Ref. 13) and the present EAM potential results. All the energies are in eV.

	SIESTA						VASP	EAM
	128_{CV}	$128+1_{CV}$	128_{CP}	250_{CV}	$250+1_{CV}$	250_{CP}	128_{CV}	2000_{CV}
Octahedral	3.04	2.87	2.77	2.94	2.85	2.81	2.97	3.38
	(0.93)	(0.96)	(1.00)		(0.94)	(0.97)	(0.97)	(0.16)
$\langle 110\rangle_{Fe\text{-}P}$	3.05	2.90	2.85	2.96	2.89	2.89	2.92	2.50
	(0.92)	(0.92)	(0.92)		(0.90)	(0.90)	(1.02)	(1.03)
Tetrahedral	3.17	3.01	2.91	3.07	2.99	2.97		2.72
	(0.80)	(0.82)	(0.86)		(0.79)	(0.82)		(0.82)
$\langle 111\rangle_{Fe\text{-}P}$	3.32	3.13	2.98	3.22	3.12	3.03	3.25	3.23
	(0.65)	(0.69)	(0.79)		(0.67)	(0.76)	(0.69)	(0.30)

and binding energies. The results are shown in Table I for various calculation conditions. The formation energies are evaluated with respect to P_{sub}, taken as the reference configuration,[7,13] and they represent the energy cost for moving a substitutional P atom to an interstitial site. The binding energy is the energy gain corresponding to the formation of a P interstitial from a Fe-Fe⟨110⟩ dumbbell and a substitutional P atom.

These energies are found to depend very weakly on the *k*-point grid, e.g., for 128-atom cells, they differ only by about 0.015 eV when increasing from a shifted $3\times3\times3$ to a shifted $5\times5\times5$ grid and keeping the same smearing width (0.3 eV). However, the dependence of P_{int} relative stabilities on the simulation cell size may be larger.[13] We have therefore evaluated the precision of the present results by performing calculations using 128- and 250-atom supercells. Three simulation conditions have been considered for each supercell size in order to compare with previous DFT results[13] and to compare their rates of convergence: (i) volume fixed to the *N*-atom bulk equilibrium volume, (ii) volume fixed to $N+1$ times the Fe atomic volume,[26,27] and (iii) constant-pressure relaxations (Table I). We note that the formation energies from 128- and 250-atom cell calculations differ by only 0.05 eV for conditions (ii) and (iii), whereas these differences are at least 0.1 eV for (i). Furthermore, the formation energies resulting from (ii) are closer to those from (iii) for both 128- and 250-atom cells. The values from (i) are systematically higher. We have used therefore 128-atom cells and the condition (ii) for the calculation of migration barriers. All the results reported below also refer to this case; the error bars in both binding and migration energies are estimated to be about 0.05 eV. The SIESTA results [128-atom cells, condition (i)] are also in good agreement with those from plane wave VASP calculations (Table I); the relative discrepancies in energies are less than 10%, attesting to the validity of the present localized basis set description of P impurities in iron.

We note that all these configurations have similar stabilities, in contrast with the SIA case,[13,20,28] and all the binding energies are rather large (Table I). The most stable configurations are the octahedral P and the ⟨110⟩ mixed dumbbell ($\langle 110\rangle_{Fe\text{-}P}$); their binding energies are, respectively, 0.96 and 0.92 eV. The energy difference between these two configurations is close to the precision limit of DFT calculations (Table I). In addition to the size difference between Fe and P atoms, the origin of the high stability of mixed dumbbell configurations may be partly due to the hybridization between the P and the Fe atom forming a dumbbell. In the case

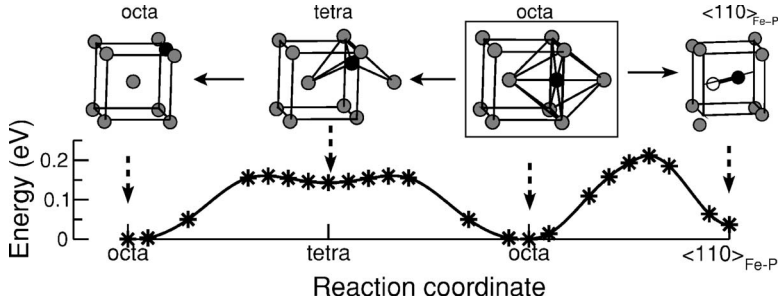

FIG. 1. *Ab initio* barriers calculated using the drag method for the jump of a P atom between two nearest octahedral sites and the transition between an octahedral and a ⟨110⟩ mixed dumbbell position. Initial, intermediate (metastable), and final configurations are schematically represented; their corresponding energy levels are indicated by dashed arrows. The P, interstitial Fe, and lattice Fe atoms (black, white, and gray spheres, respectively) are represented at their relaxed positions. The color codes for the atoms are the same in all the figures.

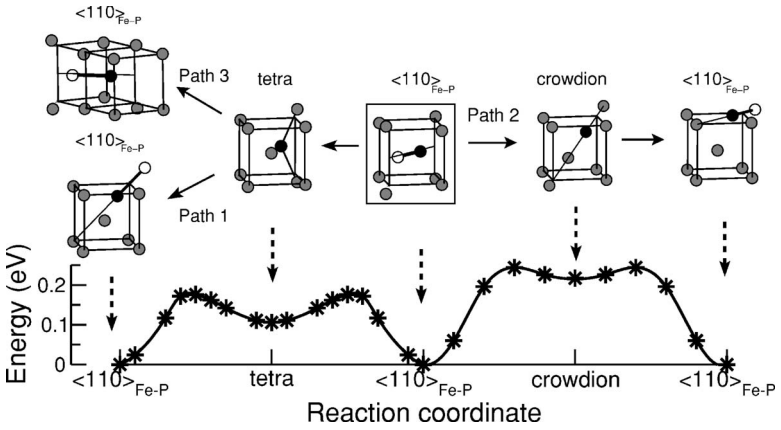

FIG. 2. *Ab initio* energy barriers obtained using the drag method for three jump mechanisms of a Fe-P ⟨110⟩ mixed dumbbell. The paths 1, 2, and 3 are the translation-rotation, the rigid translation, and the second nearest neighbor jump, respectively. Schematic representations of the initial, intermediate, and final states are shown with the atoms at their relaxed positions.

of $\langle 110\rangle_{\text{Fe-P}}$, strong hybridization exists between the $3p$ band of P and the $3d$ band of Fe, inducing local antiferromagnetism on both atoms with respect to other atoms in the bcc lattice. The magnetic moment values are $-0.2\mu_B$ for P and $-0.8\mu_B$ for Fe atoms according to Mulliken population analysis in agreement with the results in Ref. 13. The local magnetic moment of the Fe atom in a mixed dumbbell is about twice that of the Fe atom in $\langle 110\rangle_{\text{Fe-Fe}}$.

Values from *ab initio* studies are compared with those from the EAM potential by Ackland *et al.*[7] as shown in Table I. This potential also predicts the $\langle 110\rangle_{\text{Fe-P}}$ to be the lowest-energy configuration. The resulting high stabilities, i.e., large binding energies, of the ⟨110⟩ mixed dumbbell and the tetrahedral P are in good agreement with *ab initio* values. However, the octahedral P and the ⟨111⟩ mixed dumbbell are found to be less stable. These discrepancies induce some differences in the description of P migration properties as discussed below.

B. Migration of P interstitial

Concerning the migration of P interstitials, we have examined their mobilities in the two lowest configurations, the octahedral and the $\langle 110\rangle_{\text{Fe-P}}$, according to *ab initio* calculations. The P atoms are found to be highly mobile in both configurations. All the translations and rotations are two-step jumps. The initial, intermediate (metastable), and final configurations and the respective energy barriers calculated using the drag method are shown in Figs. 1–3. We note that all the jumps have similar activation energies, smaller than the migration energy of SIAs in α-iron.[20] These characteristics are consistent with the fact that the various P interstitial sites have similar stabilities.

A phosphorus atom can migrate from one octahedral site to the nearest equivalent site passing through the metastable tetrahedral position as shown in Fig. 1. The corresponding energy barrier is 0.16 eV and the migration is clearly three dimensional, i.e., the whole configurational space can be explored by successive octahedral P jumps. Note that, according to the EAM potential, the migration of octahedral P atoms will not contribute to the diffusion of P interstitials, since the octahedral site is 0.88 eV higher in energy than the $\langle 110\rangle_{\text{Fe-P}}$.

Possible translations and/or rotations of a $\langle 110\rangle_{\text{Fe-P}}$ mixed dumbbell have also been investigated in detail. The translation-rotation, the rigid translation, and the second nearest neighbor jump mechanisms are shown in Fig. 2, and the two possible on-site rotations in Fig. 3. The respective energy barriers are summarized in Table II. It is interesting to discuss the mobility of the $\langle 110\rangle_{\text{Fe-P}}$ mixed dumbbell in the light of the $\langle 110\rangle_{\text{Fe-Fe}}$ mobility in pure iron. The various $\langle 110\rangle_{\text{Fe-P}}$ jumps have similar activation energies, which are all smaller than those of the $\langle 110\rangle_{\text{Fe-Fe}}$ (Table II). In both cases, the translation-rotation is the most probable mechanism. However, the energy barrier for $\langle 110\rangle_{\text{Fe-P}}$ is 0.16 eV lower (Table II), and it passes through an intermediate tetrahedral site (Fig. 2). In addition to the translation-rotation jump, the rigid translation and the on-site rotations also contribute to the long-distance diffusion of $\langle 110\rangle_{\text{Fe-P}}$,[29] while their activation energies are too large for the $\langle 110\rangle_{\text{Fe-Fe}}$. The second nearest neighbor jump, the second most favorable jump for $\langle 110\rangle_{\text{Fe-Fe}}$, has the same energy barrier as the translation-

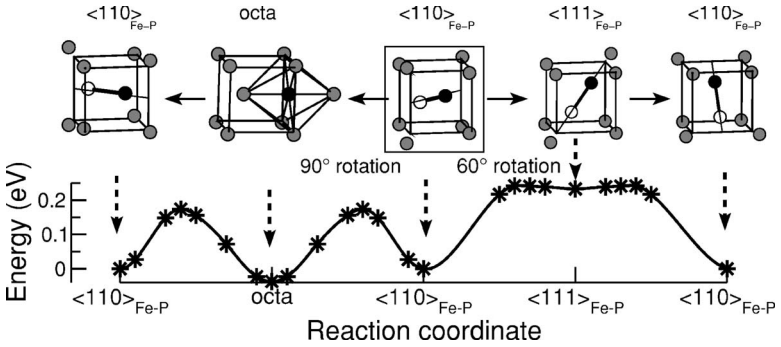

FIG. 3. Two on-site rotation mechanisms of a Fe-P ⟨110⟩ mixed dumbbell and their respective *ab initio* energy barriers calculated using the drag method.

TABLE II. Activation energies for the translation and/or rotation jumps of the Fe-Fe ⟨110⟩ and the Fe-P ⟨110⟩ mixed dumbbell in iron. Comparison between the present SIESTA and EAM potential results is shown. All energies are in eV.

	SIESTA		EAM
	$\langle 110\rangle_{\text{Fe-Fe}}$[a]	$\langle 110\rangle_{\text{Fe-P}}$	$\langle 110\rangle_{\text{Fe-P}}$
Translation-rotation	0.34	0.18	0.27
Rigid translation	0.78	0.24	
60° on-site rotation	0.56	0.24	0.72
90° on-site rotation		0.17	
Second nearest neighbor jump	0.50	0.18	
Jump to octahedral site	1.18	0.17	0.87

[a]Reference 20.

rotation jump for $\langle 110\rangle_{\text{Fe-P}}$ (Fig. 1). However, it only induces a cage movement of the P interstitial atom. A combination of this long jump with on-site rotations is required to lead to Fe-P mixed dumbbell diffusion.

The ability of empirical potentials to predict properties not included in their parameter fitting needs to be checked. In particular, the P interstitial migration barriers are compared with the more accurate *ab initio* results. Dimer method searches using the Fe-P EAM potential have been performed to study the mobility of $\langle 110\rangle_{\text{Fe-P}}$, the lowest-energy interstitial configuration according to this potential. We have also found the translation-rotation mechanism to be the most probable transition in agreement with Ref. 9; the energy barrier is 0.27 eV. The intermediate state is also the tetrahedral site as in the *ab initio* case. However, the other jumps have much higher activation energies, e.g., the energy barrier for the 60 ° on-site rotation is 0.72 eV, and the rigid translation has never been observed during 100 dimer searches. Therefore, the diffusion of $\langle 110\rangle_{\text{Fe-P}}$ occurs only via the translation-rotation mechanism according to this potential.

It is interesting to note that according to the *ab initio* calculations the transitions between octahedral P and $\langle 110\rangle_{\text{Fe-P}}$ require low activation energies: 0.17 eV for the transition from $\langle 110\rangle_{\text{Fe-P}}$ to octahedral P and 0.21 eV for the reciprocal one. These values are comparable to their respective translation and/or rotation energy barriers. Furthermore, the tetrahedral site is a common intermediate state for the migration of these two P_{int} configurations. An octahedral P may transform to $\langle 110\rangle_{\text{Fe-P}}$ when passing through a tetrahedral position, and vice versa. Therefore the two most stable and highly mobile P interstitial states are expected to interchange their configurations easily while migrating. The dissociation barriers of these two species are much higher than their respective migration barriers. Assuming the dissociation energy to be the sum of the binding energy of the P interstitial and the migration energy of $\langle 110\rangle_{\text{Fe-Fe}}$ (0.34 eV), the resulting values for octahedral P and $\langle 110\rangle_{\text{Fe-P}}$ are 1.30 and 1.26 eV, respectively.

C. Trapping of P interstitial

A fast-migrating octahedral P or a Fe-P ⟨110⟩ mixed dumbbell can get close to a substitutional P atom. The interaction between them has been shown to be strongly attractive, and various configurations containing two P atoms can be formed.[13] In this work, we only report on the lowest-energy configurations found by our *ab initio* calculations as shown in Fig. 4. Configuration (a) consists of a distorted $\langle 110\rangle_{\text{Fe-P}}$ bound to a P atom which has been pushed away from its original substitutional site along the ⟨112⟩ direction. Configuration (b) is a crowdionlike configuration where the P interstitial and Fe atoms are aligned in the ⟨111⟩ direction. Their binding energies defined with respect to an isolated Fe-P ⟨110⟩ mixed dumbbell and a substitutional P atom are, respectively, 1.05 and 1.02 eV. Note that configuration (b) is nearly unstable and easily decays to configuration (a).

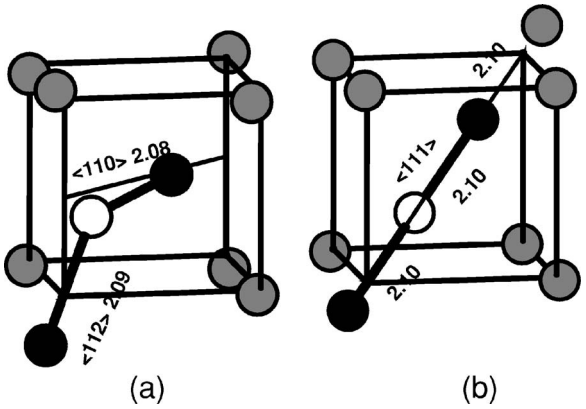

FIG. 4. Lowest-energy configurations with a P interstitial trapped by a substitutional P atom resulting in (a) P_{sub}-$\langle 110\rangle_{\text{Fe-P}}$ and (b) crowdion configuration. The atoms are at their relaxed positions. The relevant orientations and interatomic distances (in Å) are shown.

The EAM potential, which gives the correct lowest-energy migration path for $\langle 110\rangle_{\text{Fe-P}}$, also predicts configuration (a) to be the most favorable one, although the binding energy (0.29 eV) is much lower. An extensive search of possible migration paths for this two-P complex has been performed using the dimer method and this interatomic potential. The results suggest that this two-P complex cannot migrate without dissociation. The most probable dissociation path is for $\langle 110\rangle_{\text{Fe-P}}$ jumping to either the third or the fifth neighboring site of the substitutional P atom.

Based on the present *ab initio* and EAM potential studies, the fast diffusion of a P interstitial atom is therefore expected to be significantly reduced due to the formation of these highly stable and most likely immobile complexes.

D. Diffusion coefficients of SIAs and P interstitial

In order to estimate the diffusion coefficients of interstitial atoms in dilute Fe-P alloys, the transport model by Barbu and Lidiard[15] has been modified according to the present *ab initio* results. Since this model considers only the Fe-P mixed dumbbells, the contribution of P diffusion via octahedral configurations is not taken into account. However, we may expect a similar kinetic behavior from both species due to their similar stabilities and mobilities.

TABLE III. Possible interstitial atom jumps and corresponding activation energies used in the atomic transport model.

Mechanism	Jump frequency	Activation energy (eV)
$\langle 110\rangle_{\text{Fe-Fe}}$ translation-rotation	w_0	0.34
$\langle 110\rangle_{\text{Fe-P}}$ translation-rotation	w_1	0.18
$\langle 110\rangle_{\text{Fe-P}}$ rigid translation	w_1'	0.24
$\langle 110\rangle_{\text{Fe-P}}$ 60° on-site rotation	w_R	0.24
$\langle 110\rangle_{\text{Fe-P}}$ 90° on-site rotation	w_R'	0.17
$\langle 110\rangle_{\text{Fe-P}}$ dissociation	w_2	1.26
$\langle 110\rangle_{\text{Fe-P}}$ association	w_3	0.34

We have modified some analytical expressions to allow the inclusion of different jump frequencies associated with the translation-rotation and the rigid translation for both the $\langle 110\rangle_{\text{Fe-Fe}}$ and the $\langle 110\rangle_{\text{Fe-P}}$ dumbbells. Only nearest neighbor jumps are considered and we also assume that the "pair configuration" [a substitutional P atom and a $\langle 110\rangle_{\text{Fe-Fe}}$ in its nearest neighbor site] is a noninteracting configuration.

The kinetic cross coefficients D_{ij} are thus calculated in terms of the λ_{ij}:

$$D_{\text{PI}}^{\text{I}} = K(\lambda_{\text{FeFe}} + \lambda_{\text{FeP}} + \lambda_{\text{PFe}} + \lambda_{\text{PP}}), \tag{3}$$

$$D_{\text{IP}}^{\text{I}} = D_{\text{I}} + K(\lambda_{\text{FeP}} + \lambda_{\text{PP}}), \tag{4}$$

$$D_{\text{PI}}^{\text{P}} = K(\lambda_{\text{FeP}} + \lambda_{\text{PP}}), \tag{5}$$

$$D_{\text{IP}}^{\text{P}} = K\lambda_{\text{PP}}, \tag{6}$$

where $D_{\text{I}}=4a^2w_0$, $K=2\exp(E_{\text{b}}/k_{\text{B}}T)$, and

$$\lambda_{\text{FeFe}} = 2a^2w_2\left(\frac{2\left[w_1(3+2\alpha)+\frac{2}{3}w_2+w_{\text{R}}+w_{\text{R}}'\right]}{w_1(3+2\alpha)+2w_2+w_{\text{R}}+w_{\text{R}}'}-\frac{w_0}{w_3}\right), \tag{7}$$

$$\lambda_{\text{FeP}} = \frac{8}{3}a^2\left(\frac{(2+\alpha)w_1w_2}{w_1(3+2\alpha)+2w_2+w_{\text{R}}+w_{\text{R}}'}\right) = \lambda_{\text{PFe}}, \tag{8}$$

$$\lambda_{\text{PP}} = (2+\alpha)a^2w_1\left(\frac{\frac{1}{3}w_1(1+2\alpha)+2w_2+w_{\text{R}}+w_{\text{R}}'}{w_1(3+2\alpha)+2w_2+w_{\text{R}}+w_{\text{R}}'}\right), \tag{9}$$

where $\alpha=w_1'/w_1$, $2a$ is the lattice parameter of bcc iron, E_{b} is the mixed dumbbell binding energy, k_{B} is Boltzmann's constant, and T is the temperature in kelvins.

All the jump frequencies w_j are defined in Table III and they have been calculated using the associated activation energies assuming an Arrhenius behavior.

The effective diffusion coefficient of an interstitial atom, either a SIA or a $\langle 110\rangle_{\text{Fe-P}}$, can be written as

TABLE IV. Comparison between kinetic cross coefficients D_{ij} calculated with *ab initio* results and those fitted to segregation measurements from Lidiard (Ref. 14). All the D_{ij} are in 10^{-7} m^2 s^{-1}.

	Present work	Lidiard			
	D	D_{IP}^{P}	D_{PI}^{P}	D_{IP}^{I}	D_{PI}^{I}
573 K	2.1×10^{7}	5.09	6.14	8.77	11.3
523 K	9.8×10^{7}	4.90	5.72	7.69	9.65
473 K	6.3×10^{8}	4.72	5.31	6.70	8.12
423 K	6.3×10^{9}	4.55	4.95	5.84	6.79
373 K	1.2×10^{10}	4.42	4.65	5.17	5.72

$$D_{\text{I}}^{\text{eff}} = \frac{D_{\text{I}} + D_{\text{PI}}^{\text{I}}c_{\text{P}}'}{1 + Kc_{\text{P}}'} \tag{10}$$

and an effective diffusion energy of 0.19 eV has been obtained for temperatures between 373 and 723 K. At such temperatures the majority of SIAs are expected to form mixed dumbbells due to the large dissociation energy of $\langle 110\rangle_{\text{Fe-P}}$. Therefore, the low effective diffusion energy found corresponds almost to that of a $\langle 110\rangle_{\text{Fe-P}}$. This value is in good agreement with the result from Abe and Kuramoto.[30] In their resistivity recovery experiment, dilute Fe-P samples were irradiated with 2.5 MeV electrons at 77 K. A recovery stage has been observed below the uncorrelated stage I_E, i.e., before the recombination of freely migrating SIAs with vacancies from other Frenkel pairs.[31] This new stage has been proposed to be associated with the diffusion of Fe-P mixed dumbbells. According to the present *ab initio* results, the diffusion of the octahedral P may also contribute to this same stage.

We report in Table IV a comparison between the kinetic cross coefficients D_{ij} from Lidiard using the jump frequencies of Druce *et al.*[16] fitted on segregation measurements and the present values adopting the same preexponential factor (5.16×10^{12} Hz). From 373 to 573 K, the transport coefficient λ_{PP} dominates over all the others according to the *ab initio* jump frequencies. All four D_{ij} coefficients are therefore the same, and only one value D is reported. As shown in Table IV, our D coefficient is many orders of magnitude larger and has a stronger dependence on temperature than those from Lidiard. These significant differences mainly come from the large difference in the mixed dumbbell binding energies used in the two studies.

E. Kinetics of phosphorus segregation under irradiation

In view of the high stability and mobility of the Fe-P mixed dumbbells, we may expect a high dragging of P by SIAs toward grain boundaries (GBs). We have attempted to understand the intergranular segregation through this mechanism by introducing our D coefficients into the analytical expression derived by Barashev.[4] In his work, the diffusion model of Murphy and Perks has been adopted,[32] and the D coefficients are the ones fitted on the segregation measurements performed by Druce *et al.*[16] His approach is based on

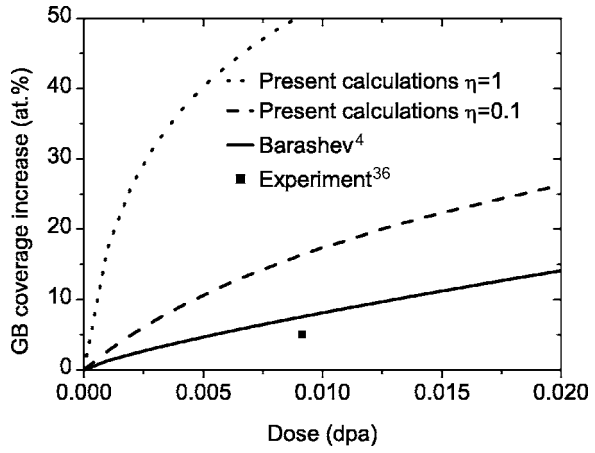

FIG. 5. Radiation dose dependence of the increase in P coverage at grain boundaries for a steel with P content $C_{P0}=6.5\times10^{-4}$ at. % at 166 °C. The available experimental value from Buswell *et al.* (Ref. 36) is also shown.

two main assumptions: the GB is an infinite sink for the solute atoms, and the solute elimination at point defect clusters in the volume is negligible. In the present study, only atomic transport of solute atoms by the interstitial mechanism is considered. The increase in the concentration of P atoms at the GB can be written as

$$\Delta C_{\mathrm{GB}}^{\mathrm{P}}(t) \approx \frac{2C_{\mathrm{P0}}}{k_{\mathrm{R}}d}\ln(1+\Gamma\eta Gt) \tag{11}$$

with

$$\Gamma = \frac{D_{\mathrm{PI}}^{\mathrm{P}}}{D_{\mathrm{I}}+D_{\mathrm{PI}}^{\mathrm{I}}C_{\mathrm{P0}}}, \tag{12}$$

where C_{P0} is the nominal atomic fraction of P atoms, G is the point defect generation rate, d is the grain boundary size, and the definition of k_{R} is given in Ref. 4. We have introduced the parameter η only to account for the fraction of free migrating point defects surviving after cascade relaxation. The values of C_{P0}, G, d, and k_{R} used here are the same as in Ref. 4.

Figure 5 shows the results assuming $\eta=1$. Our predicted grain boundary coverage of P atoms at grain boundaries increases significantly faster than that of Barashev. This is mainly due to the high binding energy of the mixed dumbbell given by *ab initio* calculation (0.92 eV) compared with 0.17 eV, the value used in Ref. 4. The increase in grain boundary coverage obtained with $\eta=0.1$, the typical value obtained by cascade molecular dynamic simulation,[33] is also reported, and the resulting curve compares better with the available experimental point. We note that η can only be equal to 1 in Barashev's work, since his D coefficients have been fitted using this value. The remaining theoretical-experimental discrepancy may be due to the following reasons: (1) The fitted parameters are obtained on real steels and not on pure FeP alloys. (2) The η parameter is smaller than 0.1. (3) A significant fraction of P atoms is trapped in stable two-P complexes or segregated on point defect clusters.

It is worth noticing that the dragging of P by interstitials is maximal ($\Gamma C_{P0}=1$) with our parameters. Furthermore, when $\mathrm{P_{int}}$ migrates through octahedral configurations, the P atom is considered to be at the same time a solute and an interstitial atom. Therefore, we also expect the corresponding P dragging to be maximal.

F. Effect of phosphorus on the nucleation of interstitial dislocation loops

In a previous study by Hardouin-Duparc and Barbu,[17] transmission electron microscopy measurements of saturated dislocation loop density were performed in Fe–0.027 at. %–P alloys irradiated with 1 MeV electrons. The result has been used to estimate the effective diffusion energy of the interstitial atoms using the Brown-Kelly-Mayer model,[34] which mainly relies on two assumptions: (i) the di-interstitial atoms are the stable nuclei of dislocation loops, and (ii) the mobility of vacancies is neglected. The dislocation loop density is then controlled by the effective diffusion coefficient of interstitial atoms ($D_{\mathrm{I}}^{\mathrm{eff}}$) as defined in Eq. (10).

The corresponding experimental effective diffusion energy (0.79 eV) is significantly larger than the value of 0.19 eV given by this work (Sec. III D). This difference can be explained by considering the formation of stable and immobile complexes containing two P atoms as discussed above (Fig. 4). Assuming the dissociation energy to be the sum of the binding energy (1.05 eV) and the effective diffusion energy (0.19 eV) of Fe-P mixed dumbbells, the resulting value is 1.24 eV. Due to the high stability of these configurations, it could therefore be taken as a first approximation to the effective migration energy of a P interstitial. This value is indeed too high compared with the experimentally derived energy barrier (0.79 eV). In order to reconcile this discrepancy, these two-P complexes need to be taken into account in both experimental data interpretation and simulation. Recently, a kinetic model has been developed for the atomic transport via interstitials in concentrated bcc alloys,[35] which may account for configurations formed by more than one solute atom.

IV. CONCLUSIONS

In summary, we have investigated the diffusion of P via interstitials in dilute FeP alloys by means of the *ab initio* SIESTA method, empirical potentials, and the atomic transport model. P atoms are found to be highly mobile in the two lowest-energy interstitial configurations, i.e., the octahedral and the ⟨110⟩ mixed dumbbell. The migration energy of the octahedral P is 0.16 eV. Both translation-rotation and rigid translation contribute to the Fe-P mixed dumbbell diffusion with migration energies of 0.18 and 0.24 eV. An effective migration energy for the Fe-P ⟨110⟩ mixed dumbbell of 0.19 eV is obtained using a modified atomic transport model. The diffusion of a P interstitial requires therefore a lower activation energy than that of a single SIA, in agreement with the results from the resistivity recovery experiments. The fast-migrating $\mathrm{P_{int}}$ atoms can be trapped by substitutional phosphorus, resulting in highly stable two-P com-

plexes. Dimer-method calculations using EAM potentials suggest that these complexes cannot migrate without dissociation; the mobility of interstitial atoms in the presence of P atoms is thus expected to be significantly reduced. The formation of these two-P complexes may be crucial to explain the high activation energy for long-distance diffusion of SIAs and P interstitial atoms according to existing experimental evidence.

ACKNOWLEDGMENTS

We acknowledge fruitful discussions with J. L. Bocquet, M. Nastar, and V. Barbe. This work was supported by the PERFECT European Integrated Project under Contract No. FI6O-CT-2003-508840. F.G. acknowledges support from the U.S. Department of Energy, Office of Fusion Energy Science under Contract No. DE-AC06-76RLO 1830.

[1] C. A. English, S. R. Ortner, G. Gage, W. L. Server, and S. T. Rosinski, ASTM Spec. Tech. Publ. **151**, 1405 (2001).
[2] Z. Lu, R. G. Faulkner, N. Sakaguchi, H. Kinoshita, H. Takahashi, and P. E. J. Flewitt, J. Nucl. Mater. **329-333**, 1017 (2004).
[3] R. G. Faulkner, S. Song, P. E. J. Flewitt, M. Victoria, and P. Marmy, J. Nucl. Mater. **189**, 255 (1998).
[4] A. V. Barashev, Philos. Mag. A **82**, 323 (2002).
[5] M. Hashimoto, Y. Ishida, R. Yamamoto, M. Doyama, and T. Fujiwara, Scr. Metall. **16**, 267 (1982).
[6] G. J. Ackland, D. J. Bacon, A. F. Calder, and T. Harry, Philos. Mag. A **75**, 713 (1997).
[7] G. J. Ackland, M. I. Mendelev, D. J. Srolovitz, S. Han, and A. V. Barashev, J. Phys.: Condens. Matter **16**, S2629 (2004).
[8] A. A. Vasiliev, V. V. Ryban, and A. A. Zisman, J. Nucl. Mater. **231**, 249 (1996).
[9] S. M. J. Gordon, S. D. Kenny, and R. Smith, Phys. Rev. B **72**, 214104 (2005).
[10] H. Hurchand, S. D. Kenny, C. F. Sanz-Navarro, R. Smith, and P. E. J. Flewitt, Nucl. Instrum. Methods Phys. Res. B **229**, 92 (2005).
[11] H. Hurchand, S. D. Kenny, and R. Smith, Nucl. Instrum. Methods Phys. Res. B **228**, 146 (2005).
[12] A. V. Barashev, Philos. Mag. **85**, 1530 (2005).
[13] C. Domain and C. S. Becquart, Phys. Rev. B **71**, 214109 (2005).
[14] A. B. Lidiard, Philos. Mag. A **79**, 1493 (1999).
[15] A. Barbu and A. B. Lidiard, Philos. Mag. A **74**, 709 (1996).
[16] S. G. Druce, C. A. English, A. J. Foreman, R. J. McElroy, I. A. Vatter, C. J. Bolton, J. T. Buswell, and R. B. Jones, ASTM Spec. Tech. Publ. **1270**, 119 (1996).
[17] A. Hardouin-Duparc and A. Barbu, MRS Bull. **439**, 509 (1997).
[18] G. Henkelman and H. Jonsson, J. Chem. Phys. **111**, 7010 (1999).
[19] J. M. Soler, E. Artacho, J. D. Gale, A. Garcia, J. Junquera, P. Ordejón, and D. Sanchez-Portal, J. Phys.: Condens. Matter **14**, 2745 (2002).
[20] C. C. Fu, F. Willaime, and P. Ordejon, Phys. Rev. Lett. **92**, 175503 (2004).
[21] C. C. Fu, J. Dalla Torre, F. Willaime, J. L. Bocquet, and A. Barbu, Nat. Mater. **4**, 68 (2005).
[22] C. C. Fu and F. Willaime, Phys. Rev. B **72**, 064117 (2005).
[23] We compared results from both methods on, e.g., the translation-rotation migration path of the ⟨110⟩ mixed dumbbell using the Fe-P EAM potential. The agreement is excellent and the discrepancy in the saddle point energy is less than 0.001 eV, which is negligible compared with other possible errors.
[24] F. Gao, G. Henkelman, W. J. Weber, L. R. Corrales, and H. Jonsson, Nucl. Instrum. Methods Phys. Res. B **202**, 1 (2003).
[25] A. R. Allnatt and A. B. Lidiard, *Atomic Transport in Solids* (Cambridge University Press, Cambridge, UK, 1993).
[26] F. Willaime, J. Nucl. Mater. **323**, 205 (2003).
[27] The Fe and the P atomic volumes in the bcc iron lattice are assumed to be the same due to the very small lattice distortion induced by a substitutional P.
[28] C. Domain and C. S. Becquart, Phys. Rev. B **65**, 024103 (2001).
[29] J. L. Bocquet, Philos. Mag. A **63**, 157 (1991).
[30] H. Abe and E. Kuramoto, J. Nucl. Mater. **271-272**, 209 (1999).
[31] S. Takaki, J. Fuss, H. Kugler, U. Dedek, and H. Schultz, Radiat. Eff. **79**, 87 (1983).
[32] S. M. Murphy and J. M. Perks, J. Nucl. Mater. **17**, 360 (1990).
[33] D. J. Bacon, F. Gao, and Y. N. Osetsky, J. Nucl. Mater. **276**, 1 (2000).
[34] L. M. Brown, A. Kelly, and R. M. Mayer, Philos. Mag. **19**, 721 (1969).
[35] V. Barbe and M. Naster (unpublished).
[36] J. T. Buswell, C. J. Bolton, M. R. Wooton, P. E. J. Bischler, R. B. Jones, L. T. Jones, W. J. Phythian, and R. Sinclair, ASTM Spec. Tech. Publ. **1175**, 332 (1993).